

Prediction of Emperor-Hawaii seamount locations from a revised model of global plate motion and mantle flow

Bernhard Steinberger^{1*}, Rupert Sutherland² & Richard J. O'Connell³

¹*Institute for Frontier Research on Earth Evolution (IFREE), Japan Agency for Marine-Earth Science and Technology (JAMSTEC) (previously Japan Marine Science and Technology Center), 2-15 Natsushima-cho, Yokosuka 237-0061, Japan*

²*Institute of Geological and Nuclear Sciences, PO Box 30-368, Lower Hutt, New Zealand*

³*Department of Earth and Planetary Sciences, Harvard University, 20 Oxford Street, Cambridge, Massachusetts 02138, USA*

* Present address: Bayerisches Geoinstitut, Universität Bayreuth, D-95440 Bayreuth, Germany. After 1 August 2004: Norges geologiske undersøkelse, N-7491 Trondheim, Norway

The bend in the Hawaiian-Emperor seamount chain is a prominent feature usually attributed to a change in Pacific plate motion ~47 Myr ago. However, global plate motion reconstructions fail to predict the bend. Here we show how the geometry of the Hawaiian-Emperor chain and other hotspot tracks can be explained when we combine global plate motions with intraplate deformation and movement of hotspot plumes through distortion by global mantle flow. Global mantle flow models predict a southward motion of the Hawaiian hotspot. This, in combination with a plate motion reconstruction connecting Pacific and African plates through Antarctica, predicts the Hawaiian track correctly since the date of the bend, but predicts the chain to be too far west before it. But if a reconstruction through Australia and Lord Howe rise is used instead, the track is predicted correctly back to 65 Myr ago, including the bend. The difference between the two predictions indicates the effect of intraplate deformation not yet recognized or else not recorded on the ocean floor. The remaining misfit before 65 Myr ago can be attributed to additional intraplate deformation of similar magnitude.

Hotspots are frequently assumed to be fixed and used as a reference frame for plate motions¹. However, when the Hawaiian hotspot track is predicted from a global plate motion chain based on relative plate motion data, and it is assumed that the Hawaiian hotspot is fixed relative to African hotspots, it does not fit the observed track: the predicted track is essentially straight, lies south of the Hawaiian seamount chain, and has no feature corresponding to the Hawaiian-Emperor bend². Explanation of this misfit requires one of the following, or a combination of them, to be true: (1) motion of Pacific plate hotspots, in particular more than 1,000 km southward motion for the Hawaiian hotspot between ~80 Myr ago and the time of the bend and minor southward motion after this time, (2) motion of hotspots in the African hemisphere, (3) motion at an additional plate boundary, or (4) deformation at a diffuse intraplate boundary not included in the plate motion chain. Palaeomagnetic data from the Emperor chain³ yield a southward component of Hawaiian hotspot motion more than 1,000 km relative to the palaeomagnetic axis between ~80 and 49 Myr ago. True polar wander⁴ can explain at most a small fraction of this motion. Hence the southward component of hotspot motion required by palaeomagnetic data is roughly the same as the southward component required to remove the misfit between the observed Hawaiian hotspot track and the track predicted by the plate motion chain². However, to remove the misfit before the bend by solely invoking Pacific plate hotspot motion additionally requires a westward component of Hawaiian hotspot motion; to explain the sharp bend would further require that this motion slowed down abruptly at the time of the bend.

Here we use a model of plumes moved and distorted by global mantle flow to compute hotspot motion, and combine it with plate motions to predict hotspot tracks globally. We show that computed hotspot motion is sufficient to remove any misfit between predicted and observed tracks after the time of the Hawaiian-Emperor bend. Initial radiometric dating of seamounts near the bend yielded ages of ~43 Myr⁵, but recent work suggests that it might be as old as

50 Myr⁶. For the track before the time of the bend we use two different plate motion chains connecting Pacific and African plates. With chain model 1, which goes through Antarctica, the Hawaiian track before the bend, as well as the bend itself, is not correctly predicted. None of our plume motion models yield the westward component of motion of the Hawaiian hotspot that is required for a correct prediction. However, with chain model 2, which goes through Australia and the Lord Howe rise, the bend and the Hawaiian hotspot track for times between 65 Myr ago and the present is predicted.

We restrict our discussion to four hotspots: Hawaii and Louisville in the Pacific hemisphere, and Tristan and Réunion in the African hemisphere. These are both necessary and sufficient for the purpose of this paper. They are necessary because at least two hotspots on each plate are needed to separately determine plate motions relative to hotspots in either hemisphere. They are sufficient because we show that it is not possible to fit these four tracks simultaneously with plate motion chain model 1 at times before the Hawaiian-Emperor bend. Moreover, we have shown previously⁷ that, separately for each hemisphere, a greater number of hotspot tracks can be fitted by our model results that predict hotspot motion. On the basis of circumstantial evidence, these four hotspots are among the seven most likely candidates for a deep mantle origin⁸—an underlying assumption of our model. The three others are probably not suitable for the purpose of this paper: the Easter plume is important for the question of hotspot motion during the past ~47 Myr but not so important for the time before that⁹; the Iceland plume might not have left a clear 'hotspot track'—instead, volcanic features in the region might be caused by plume-ridge interaction¹⁰; and the Afar hotspot probably initiated less than 47 Myr ago¹¹⁻¹⁴.

Hotspot motions predicted by mantle flow models

We compute hotspot motion with a method that was developed and described in detail previously¹⁵. Results shown here are for one

particular model; however, comparison with our previous work^{7,9,15–17} shows that these are typical results. By referring to these previous results, we show that the conclusions here do not depend on the choice of one particular set of model parameters but are robust conclusions that are valid as long as our model is at least

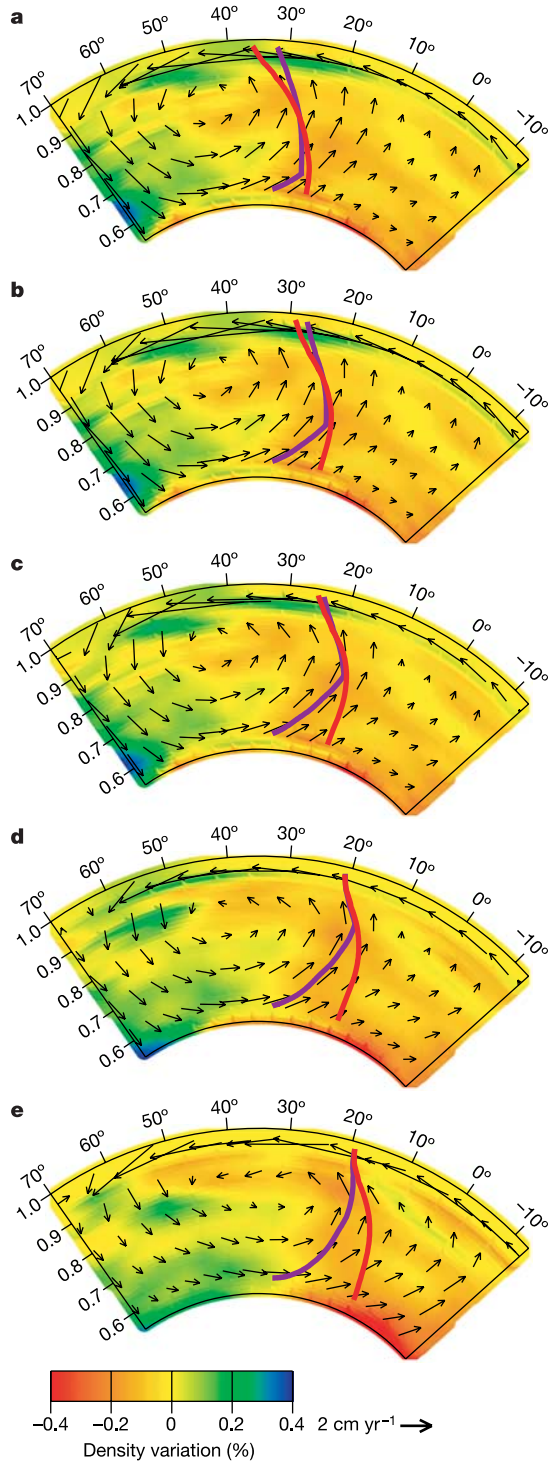


Figure 1 North–south mantle cross-section at 155° W. For different times, computed mantle density anomalies are shown in rainbow colours, and north–south and vertical components of computed mantle flow as arrows. **a**, 120 Myr ago; **b**, 90 Myr ago; **c**, 60 Myr ago; **d**, 30 Myr ago; **e**, present. Also shown is the projection of the predicted Hawaiian plume conduit for source moving with the flow (plume initiation age 170 Myr ago; thick red line) and fixed source (age 150 Myr ago; thick violet line) at those times.

qualitatively correct. The computation consists of two steps. First, a large-scale mantle flow field is computed, which is based on a mantle density structure inferred from seismic tomography, global plate motions and a radial mantle viscosity structure; this model fits several observational constraints (see Supplementary Information 1). The computed large-scale flow field is time dependent, although it does not change much over the period considered here. In the lower part of the mantle, the computed flow field is dominated by structure of spherical harmonic degree two, with large upwellings under the Pacific Ocean and Africa, downwellings around the Pacific Ocean, and flow towards the large upwellings in the lowermost mantle. In the upper part of the mantle, flow is also related to plate motions. In the uppermost part of the lower mantle, computed flow is a combination of outward flow away from the large upwellings and plate return flow towards ridges. The latter might be an important contribution close to spreading ridges. Figure 1 shows a cross-section through density and flow field for different times beneath the Pacific Ocean.

In the second step, a plume conduit is inserted into the flow field. It is taken to be initially vertical. Plume initiation times are assumed to be the same as in ref. 7, except for Hawaii, where the age is unknown and 170 or 150 Myr ago is used here. The base of the plume (assumed at depth 2,620 km, at the top of a low-viscosity layer) is assumed either to move with the horizontal component of flow or to be fixed in location (see Supplementary Information 1). The velocity of points along the plume conduit is computed as the vector sum of ambient mantle flow and a buoyant rising velocity (see Supplementary Information 1). It is assumed that plume conduits do not influence larger-scale mantle flow. Hotspot surface motion is computed from the positions where, over time, the plume conduit reaches the base of the lithosphere (assumed at depth 100 km). Our choice of modelling parameters and assumptions has been explained in previous work^{7,9,15,16}.

Motion of plume conduits in a high-viscosity lower mantle is dominated by advection, and in a low-viscosity upper mantle it is dominated by buoyant rising. Consequently, hotspot motion tends to be similar to the horizontal flow component at the depth at which the transition from low to high viscosity occurs (that is, the upper part of the lower mantle)¹⁶. For the viscosity structure used, the horizontal flow at this depth has a root-mean-square value of $\sim 1 \text{ cm yr}^{-1}$. Beneath the Tristan and Réunion hotspots it is dominated by outward flow from the large upwelling under Africa; in the case of Louisville it is a combination of flow away from the large upwelling under the Pacific Ocean and plate return flow towards the Pacific–Antarctic ridge¹⁷. The computed motion of these hotspots is indeed slow and is as expected from the flow pattern (Fig. 2). For the Hawaiian plume, another effect leads to faster (a few cm yr^{-1}) hotspot motion. Figure 1 shows a projection of the Hawaiian conduit; it is strongly tilted in a north–south direction. Flow in the upper part of the mantle is to the north and in the lower part to the south, which tilts and distorts the plume. Subsequently, the rising of a tilted plume conduit, aided by a large-scale upwelling, causes comparatively rapid hotspot motion. Among the hotspots considered here, we find this effect only for the Hawaiian hotspot.

We have previously shown results for a larger number of models, and discussed the dependence of results on various model parameters^{7,9,15–17}. In summary, these results yield the following. For Hawaii, the motion is in a southerly to southeasterly direction. The average speed is moderately slow ($\sim 1 \text{ cm yr}^{-1}$), but episodes of faster motion (several cm yr^{-1}), lasting for several tens of Myr occur for some models. Computed hotspot motion tends to be faster, if an older age for the plume is assumed. For Louisville there is slow motion ($\sim 1 \text{ cm yr}^{-1}$ or less) in various directions—in most cases in a southeasterly direction. For Réunion there is slow motion ($\sim 1 \text{ cm yr}^{-1}$ or less) in an easterly direction. For Tristan there is either very slow motion (less than 1 cm yr^{-1}) in a southeasterly to southwesterly direction, or an almost stationary hotspot.

Obviously, it is also possible to construct models with substantially larger hotspot motion (for example, with lower viscosity, and/or larger density anomalies in the mantle¹⁵); however, such models are not consistent with observations, such as hotspot tracks, whereas the models just summarized are broadly consistent. The directions of hotspot motion are less sensitive to model differences than are the speeds of motion.

Relative plate motions and hotspot tracks

We now account for predicted hotspot motion and compute hotspot tracks from specified relative plate motions. We cannot give formal uncertainties, although—on the basis of the spread of model results as just discussed—we can judge whether a discrepancy seems to be significant. The global tectonics of the Earth is characterized by a group of plates that diverge from the Indian and Atlantic oceans, and a Pacific group of oceanic plates that converge around most of

the Pacific rim. The relative motions of the two groups can be determined from observations of the sea floor in the South Pacific and southern Indian Ocean, with the caveat that deformation is known to have occurred in continental regions of Antarctica and New Zealand, but this is hard to quantify.

For times younger than chron 20 (43 Myr ago), substantial Australia–Pacific plate motion (through New Zealand) cannot be determined with sufficient precision from local data for it to be useful in this analysis. However, seafloor spreading in the South Pacific is accurately quantified¹⁸, and motion between East and West Antarctica has been determined from a consideration of seafloor geometry¹⁹. The motion of Africa, relative to East Antarctica since the Late Cretaceous, is determined from sea floor in the Southwest Indian Ocean²⁰. Hence the motion of Africa relative to the Pacific plate is determined by a plate motion chain running from Africa through East Antarctica and West Antarctica to the Pacific (Figs 3, 4).

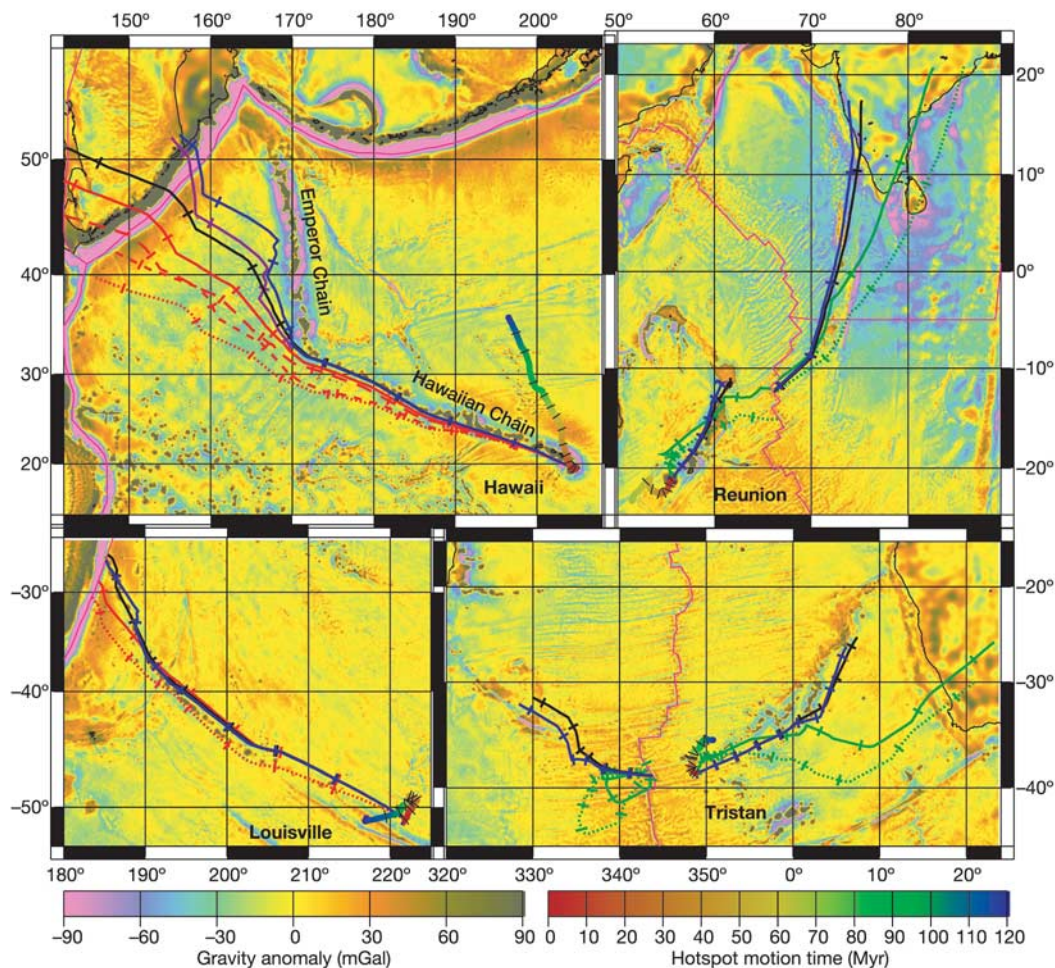


Figure 2 Computed hotspot motion and tracks for the moving-source model. Hotspot motion is shown as rainbow-coloured lines (right colour bar), tracks as single-coloured lines (shown for the past 83 Myr); tickmark interval is 10 Myr for both. Hotspot tracks are computed for the motion of the plate where they are located, except for Hawaii, where tracks computed for motion of the Pacific plate are plotted beyond its boundary. Tracks are plotted regardless of whether a hotspot was actually beneath a given plate at a given time. Red lines (model 1, shown for Hawaii and Louisville), and the purple line (model 2, shown for Hawaii), are computed for absolute plate motions such that the fit to Tristan and Réunion hotspot tracks is optimized for the two plate motion chain models as indicated; optimization parameters are African plate rotations 0–47 and 47–83 Myr ago. Green lines (shown for Réunion and Tristan) are for optimizing the fit to Hawaii and Louisville for plate motion chain model 1; parameters are Pacific plate rotations 0–25, 25–47, 47–62 and 62–83 Myr ago. Black (model 1) and blue (model 2) lines are for optimizing jointly to all

four tracks for the two plate motion chain models as indicated; parameters are African rotations 0–47, 47–62 and 62–83 Myr ago. Dotted lines, hotspots assumed fixed; short-dashed line, only hotspot motion on African hemisphere considered (shown for Hawaii); long-dashed line, only hotspot motion on Pacific hemisphere considered (shown for Hawaii); continuous lines, all hotspot motions considered. A least-squares method⁷ is used to optimize the fit to locations and radiometric ages (see Fig. 5) of seamounts. Free air gravity⁴⁴ shows actual hotspot tracks. This, rather than topography, was chosen because it should better distinguish between actual hotspot tracks (that is, seamounts formed above a plume, in an intraplate location) and material erupted at a ridge through plume–ridge interaction: the former are not expected to be in isostatic equilibrium and should therefore be readily visible on a gravity map. The latter is expected to be approximately in isostatic equilibrium, hence without strong gravity signature.

For times between chrons 24 and 34 (52–83 Myr ago), it is possible to determine Africa–Pacific relative motion by using the same geometrical connection through Antarctica (model 1), but substantial uncertainty surrounds the nature of intra-Antarctic deformation. In model 1 we assume that there was no Antarctic deformation before 43 Myr ago. An alternative plate motion chain through Australia–East Antarctica is possible (model 2) and might be more reliable. Australia–East Antarctica motion is known from data in the Southeast Indian Ocean²¹. Lord Howe rise–Australia motion is quantified back to an age of chron 33y (73 Myr ago) from Tasman Sea data²². Total Pacific–Lord Howe rise motion since the cessation of spreading in the Tasman Sea (shortly after chron 24) is accurately quantified by fitting rifted oceanic margins south of New Zealand²³. Magnetic anomaly 18 is the oldest anomaly identified in the southeast Tasman Sea²⁴. Stratigraphic evidence, combined with extrapolation of southeast Tasman Sea spreading rates to the rift margin, provides a best fit for the inception of the Eocene Lord Howe rise–Pacific (Campbell plateau) plate boundary at about chron 20^{23,24}. This is also about the time that the Adare basin was formed¹⁹, and the time of most rapid change in the southeast Indian Ocean²¹. For these reasons we choose in model 2 to switch from a West Antarctic relative motion chain at chron 20 to an Australia

relative motion chain at chron 21, and interpolate linearly for times between chrons 20 and 21.

We compute predicted hotspot trails by using both relative plate motion chains and best-fitting ‘absolute’ plate motions in the mantle reference frame⁷. Relative plate motions are listed in

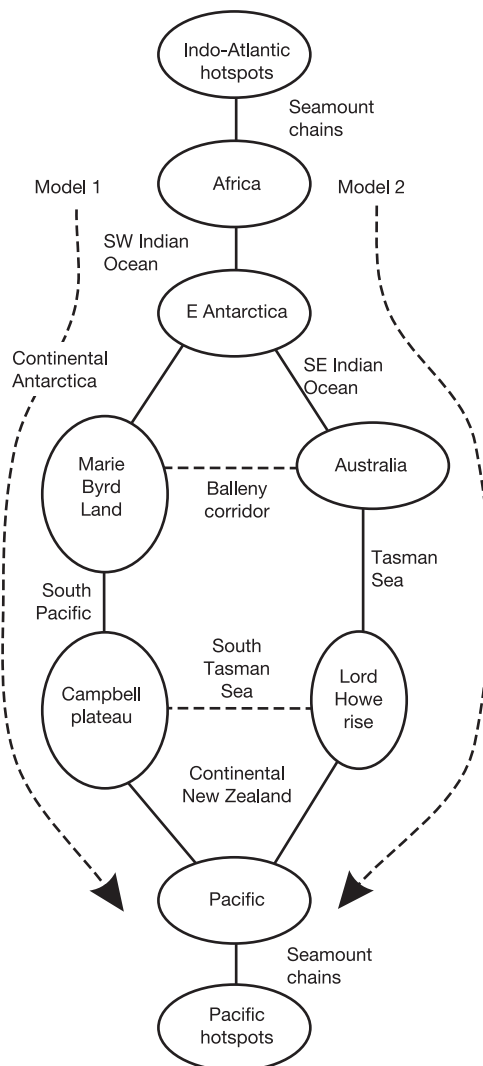


Figure 3 Diagram showing relative plate motion chains considered for times older than chron 20 (43 Myr ago). For times younger than chron 20, models 1 and 2 each follow a chain passing through continental Antarctica. The closed loop in the centre is the South Pacific plate motion circuit. Relative plate motions are listed in Supplementary Table S1.

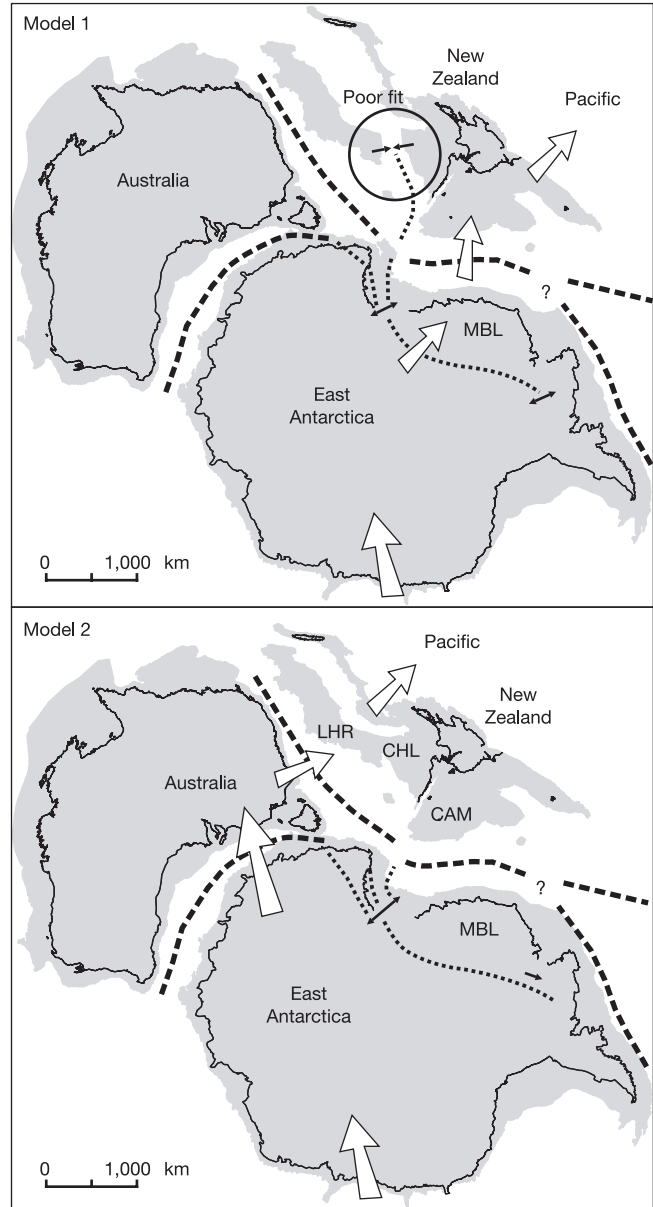


Figure 4 South Pacific reconstructions at chron 31y (68 Myr ago). Present-day coastlines and continental slopes shallower than 2,000 m (shaded) are shown for reference. Open arrows show geographic paths of plate motion chains (Fig. 3). Dashed lines are divergent plate boundaries with seafloor spreading. Dotted lines are inferred intracontinental plate boundaries required to accommodate plate-circuit closure. In model 1, intra-Antarctic motion is specified¹⁹ and residual motion before 43 Myr ago is accommodated within New Zealand. In model 2, residual motion before 43 Myr ago is accommodated within Antarctica. The large convergence required in New Zealand by model 1 during the interval 74–47 Myr ago is inconsistent with geological observations of low sedimentation rate and undeformed stratigraphy overlying rifted basement. In model 2, the total intra-Antarctic plate motion in the Ross Sea is about 300 km of rifting, with required motion becoming smaller and more dextral-oblique to the south and east (finite rotation is 79.7° S, 56.1° W, 6.7°). This is consistent with regional observations. Plate motion arrows in New Zealand and Antarctica are scaled to be double the predicted motion. LHR, Lord Howe rise; CHL, Challenger plateau; CAM, Campbell plateau; MBL, Marie Byrd Land.

Supplementary Table S1. The greatest uncertainty in model 2 lies in the possibility that a plate boundary existed through New Zealand, where there is evidence for minor rifting²⁵. If a through-going Pacific–Lord Howe rise boundary existed and had significant motion, it must have connected to the Pacific–Antarctic ridge southeast of New Zealand. We cannot rule this out, but note that South Pacific seafloor data place a moderately strong constraint on the possible existence of such a boundary for times younger than chron 33y (73 Myr ago) and previous reconstructions of seafloor data have not required one^{18,26}. Deformation in New Zealand is discussed further below.

Model 1: plate motion chain through Antarctica

If we assume fixed hotspots we obtain misfits as previously found^{2,18,27} (dotted red and green lines in Fig. 2). If hotspot motion is considered we obtain the continuous lines. The difference between dotted and continuous lines comes from both hotspot motion in the Pacific (to a greater part) and African (to a lesser part) hemisphere. This is illustrated for the Hawaiian track, for which we also show predictions that separately consider African hotspot motion (short-dashed line) and Pacific hotspot motion (long-dashed line). Hotspot motion in the Pacific and in the African hemisphere tends to move the predicted track in the right direction; for the model shown here, the combined effect is about the right magnitude. Hence we reiterate our previous conclusion¹⁶ that, within the uncertainties of our model, hotspot motion (and in particular, motion of the Hawaiian hotspot) is sufficient to explain any discrepancies between predicted and observed tracks during the

past ~47 Myr, and no ‘missing links’ in the plate motion chain are required.

However, the situation is different before 47 Myr ago, because the predicted Hawaiian track (continuous red line) shows no sign of a bend: predicted locations before 47 Myr ago are too far west. To eliminate that misfit we would need a strong westward component of Hawaiian hotspot motion, in addition to the predicted southward motion. However, none of our models yield such a motion: the computed geometry of large-scale flow in the vicinity of the Hawaiian hotspot, and hence its motion (which is consistently towards the south or southeast in most of our model results) is a consequence of its location between the large upwelling under the Pacific south of Hawaii and regions of past subduction in the north Pacific. Because of the simple geometry of the flow field, there is no reason for a westward component of Hawaiian hotspot motion. The green continuous lines show that computed motion of hotspots in the African hemisphere is equally insufficient to eliminate the misfit: particularly for the Tristan hotspot, a strong additional eastward component of motion would be required before 47 Myr ago, and none of our models yield such a motion—all models yield slow hotspot motion, and not in an eastward direction. The black lines show that a combination of additional westward Hawaiian hotspot motion and eastward Tristan hotspot motion would produce a better fit, but this combination is similarly unlikely.

Model 2: plate motion chain through Australia

Hotspot tracks computed with a plate motion chain through Australia for the interval 83–52 Myr ago are shown as the blue lines in Fig. 2. Although predicted slightly too far west, the northerly trend of the younger part of the Emperor seamount chain is now adequately reproduced, as is the prominent Emperor–Hawaii bend. Palaeolatitudes are predicted well³, but the predicted Hawaiian track before ~65 Myr ago is still west of the actual location of the northern Emperor chain.

For Louisville, Tristan and Réunion, the fit is now very good, and the predicted position of the Tristan track 80 Myr ago is close to the location that presumably marks the ridge crossing²⁸. Tristan and Réunion hotspots have been close to spreading ridges, so that volcanics along their tracks might partly represent flow towards ridges and not eruption above the plume stem^{28,29}. Although uncertainties of hotspot motion cannot be formally quantified, we suggest that any remaining misfit can be attributed to a lateral flow of plume material and inaccuracies associated with the computation of hotspot motions and plate reconstructions. The northern Emperor chain is the only possible exception, where predictions are significantly west of observed locations. Figure 5 shows that this model also yields a good fit to observed age progressions along hotspot tracks, with the exception of the northern Emperor chain. Other misfits might be partly due to inadequate age dates, and might again be partly explained by a lateral flow of plume material and inaccuracies in modelled hotspot motion. For example, a better fit for the Louisville hotspot would be achieved for somewhat faster hotspot motion, still within the range of modelling results obtained¹⁷.

Deformation 65–47 Myr ago

The difference between the predictions of plate motion chain models 1 and 2 is entirely the effect of intraplate deformation not recorded on the ocean floor. For the interval 65–47 Myr ago, the ‘missing’ motion that is required within the closed South Pacific plate-motion circuit is most probably within Antarctica. The implied deformation requires relative motion about a local rotation pole, such that rifting in the Ross Sea diminishes rapidly southwards (Fig. 4). There is abundant evidence for such a deformation.

Geophysical investigations in Antarctica reveal a broad (~1,200-km) region of extended crust adjacent to the Transantarctic Mountains that can be traced through the Ross Sea and southern Marie

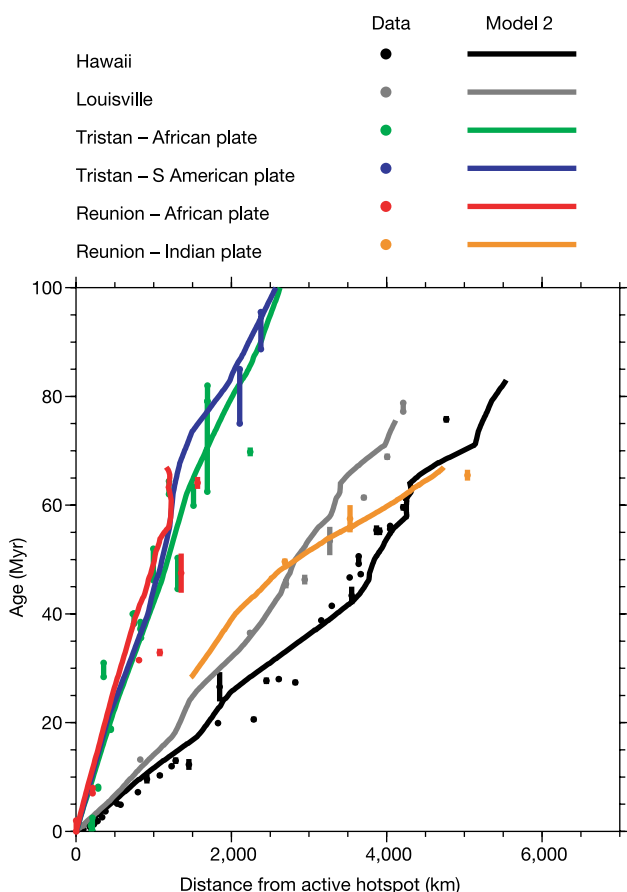


Figure 5 Age progression along hotspot tracks. Lines are for model 2; dots are available age dates, compiled for Hawaii^{3,5,6}, Louisville^{45,46}, Réunion^{47,48} and Tristan^{49,50}. Some of these sources are themselves compilations, which cite original references. Colours represent hotspot tracks as indicated.

Byrd Land^{30,31}. Farther east, the adjacent Thurston Island and Antarctic peninsula regions contain evidence for dextral oblique convergence and subduction-related volcanism that persisted until Oligocene time^{32,33}. The observed geometry of crustal strain is best approximated by a clockwise motion of Marie Byrd Land, relative to East Antarctica, about a local rotation pole near the Weddell Sea³³.

Crustal thickness results from the central Ross Sea imply 350–400 km of extension, which could be revised to 400–450 km if some volcanic addition to the crust were allowed for³⁰. When combined with the Adare trough data, the result suggests that 60–70% of Ross Sea extension occurred before ~50 Myr ago. Seafloor analyses show that some deformation occurred in the northern Ross Sea during the interval 65–47 Myr ago³⁴. Additional motion might have partly transferred to the Tasman–Pacific ridge, through the Emerald Fracture zones. Reconstructions of the Southeast Indian Ocean indicate that deformation might have occurred in the Northern Victorialand–South Tasman rise region²¹. If an alternative hypothesis is considered, namely that deformation was instead within New Zealand, then the required convergent deformation is found to be quite inconsistent with known structure of the region^{25,35–37} (Fig. 4).

Deformation 83–65 Myr ago

Deformation in New Zealand can help to explain the remaining misfit for the oldest part of the Emperor chain: the plate motion chains used in both models 1 and 2 pass through the New Zealand continent and therefore might be affected by unquantified New Zealand deformation. For times younger than chron 27 (61 Myr ago), it has been shown that South Pacific sea floor is consistent with spreading at a single ridge, and hence New Zealand deformation is not significant¹⁸. However, for times older than chron 27, it is known that South Pacific ocean crust is not consistent with a two-plate system¹⁸. In part, this is very likely to be the result of separate motion of the Bellingshausen plate adjacent to Antarctica^{26,38}, which does not affect our conclusions, but some ambiguity exists whether New Zealand deformation is also possible. It has been suggested on geological grounds²⁵. For the interval immediately after the breakup of New Zealand and Antarctica (83–74 Myr ago), there is little doubt that some New Zealand deformation took place^{25,35}. If that deformation is described by a rotation pole anywhere near eastern New Zealand, as suggested by observations of geological and crustal structure, then the effect of including it will be to improve the fit of the older part of model 2. We suggest that at least some of the misfit of the older part of the Emperor seamount chain is associated with as yet unquantified motion within New Zealand, and the subject merits more detailed investigation.

Recent results³⁹ also show that ultraslow spreading is characterized by a lack of transform faults and mantle is emplaced to the sea floor over large regions. Thus, a characteristic magnetic stripe pattern cannot be expected either. It is therefore possible that real uncertainties of plate reconstructions, and real amounts of extension, in regions characterized by very slow divergence are larger than those obtained from formal error analysis. With somewhat larger amounts of Antarctic and New Zealand deformation we could reduce the misfit to an insignificant level. A wide range of models—with deformation axes anywhere within the deformed regions—is adequate to explain hotspot tracks.

The Hawaiian–Emperor bend

Our model 2 explicitly includes a major change in relative plate motions during the interval 43–52 Myr ago. Our computations suggest that, relative to the deeper mantle beneath, the Pacific plate, not the African plate, changed its motion around this time, thus causing the bend in the Hawaiian–Emperor chain¹⁶. The mechanism by which the implied change in force balance was achieved so rapidly remains an important question in geodynamics.

Calculated tractions on the lithosphere, based on a very similar mantle flow model as used for calculating hotspot motion, show a

pattern consistent with the proposed deformation (see Supplementary Information 2). Rapid formation of oceanic lithosphere adjacent to Antarctica after the time of the Emperor–Hawaii bend might be partly responsible for the changing style of Antarctic deformation at around that time. Continental lithosphere deforms more easily than oceanic lithosphere (see, for example, ref. 40 and references therein) and the formation of stronger oceanic lithosphere surrounding Antarctica after ~50 Myr ago might have caused stress concentration and localization of deformation in the Adare basin; this might eventually have caused deformation to stop. The resulting change in the force balance of the Pacific plate, which was smaller at that time, might have been sufficient to initiate subduction in the Izu–Bonin–Mariana trench⁴¹, which might have further accelerated the change in direction of Pacific plate motion.

Discussion

An attempt to explain hotspot tracks globally by intraplate deformation alone, without hotspot motion, is not sufficient, because it would require rotations describing motion within Antarctica or New Zealand that have rotation poles far from the respective regions. Such predictions are not consistent with regional observations. However, the inclusion of hotspot motion associated with the computed plume advection makes it possible to explain hotspot tracks with axes of deformation that lie within the deformed regions, which is consistent with formal uncertainties¹⁹ and geodynamic considerations⁴². Neither hotspot motion nor intraplate deformation alone offers a suitable explanation for the set of global observations; only a combination of the two does so.

The nature of the models and observations makes a formal analysis of error difficult, but the success of the models in reconciling hotspot tracks and plate motions for times since 47 Myr ago, and also the correspondence of the model with palaeolatitudes of older parts of the Hawaiian track³, give it much credence. The case for the cause of the bend in the Hawaiian–Emperor track rests on the comparison of plate motion chains through Australia–Lord Howe rise and East–West Antarctica, where there is a clear discrepancy. This is best explained by East–West Antarctica motion before 47 Myr ago. Such intraplate deformation is roughly consistent with geological evidence and could be associated with additional oceanic deformation that might be hard to identify. Future work might better identify the nature of the deformation in the region and allow testing of the hypothesis presented here. In addition, the models that predict hotspot motion are based on seismic models of mantle heterogeneity, which are limited in resolution, and also on geodynamical assumptions relating seismic properties to density anomalies and mantle flow. These models will certainly improve as better data and more geodynamical constraints, such as reliable images of mantle plumes, become available. Nevertheless, the model we have proposed is plausible, it offers a coherent explanation of observed hotspot tracks, and it is consistent with a wide range of global observations. □

Methods

Figures were prepared using the GMT software⁴³.

Received 4 March; accepted 12 May 2004; doi:10.1038/nature02660.

1. Morgan, W. J. Deep mantle convection plumes and plate motions. *Am. Assoc. Petrol. Geol. Bull.* **56**, 203–213 (1972).
2. Molnar, P. & Stock, J. Relative motions of hotspots in the Pacific, Atlantic and Indian oceans since late Cretaceous time. *Nature* **327**, 587–591 (1987).
3. Tarduno, J. A. *et al.* The Emperor Seamounts: A record of southward motion of the Hawaiian hotspot plume in Earth's mantle. *Science* **301**, 1064–1069 (2003).
4. Besse, J. & Courtillot, V. Apparent and true polar wander and the geometry of the geomagnetic field in the last 200 million years. *J. Geophys. Res.* **107**, 2300 doi:10.1029/2000JB000050 (2002).
5. Clague, D. A. & Dalrymple, G. B. in *The Eastern Pacific Ocean and Hawaii*, vol. N of *The Geology of North America* (eds Winterer, E. L., Hussong, D. M. & Decker, R. W.) 188–217 (GSA, Boulder, CO, 1989).
6. Sharp, W. D. & Clague, D. A. An older, slower Hawaii–Emperor bend. *Eos* **83** (Fall Meet. Suppl.) Abstract T61C-04 (2002).

7. Steinberger, B. Plumes in a convecting mantle: models and observations for individual hotspots. *J. Geophys. Res.* **105**, 11127–11152 (2000).
8. Courtillot, V., Davaille, A., Besse, J. & Stock, J. Three distinct types of hotspots in the Earth's mantle. *Earth Planet. Sci. Lett.* **205**, 295–308 (2003).
9. Steinberger, B. Motion of the Easter Island hotspot relative to hotspots on the Pacific plate. *Geochem. Geophys. Geosyst.* **3**, 8503 doi:10.1029/2002GC000334 (2002).
10. Vink, G. E. A hotspot model for Iceland and the Voring Plateau. *J. Geophys. Res.* **89**, 9949–9959 (1984).
11. Hofmann, C. *et al.* Timing of the Ethiopian flood basalt event and implications for plume birth and global change. *Nature* **389**, 838–841 (1997).
12. Rochette, P. *et al.* Magnetostratigraphy and timing of the Oligocene Ethiopian traps. *Earth Planet. Sci. Lett.* **164**, 497–510 (1998).
13. Coulie, E. *et al.* Comparative K-Ar and Ar/Ar dating of Ethiopian and Yemenite Oligocene volcanism: Implications for timing and duration of the Ethiopian Traps. *Earth Planet. Sci. Lett.* **206**, 477–492 (2003).
14. Courtillot, V. & Renne, P. On the ages of flood basalt events. *C.R. Geosci.* **335**, 113–140 (2003).
15. Steinberger, B. & O'Connell, R. J. Advection of plumes in mantle flow: implications for hotspot motion, mantle viscosity and plume distribution. *Geophys. J. Int.* **132**, 412–434 (1998).
16. Steinberger, B. & O'Connell, R. J. in *The History and Dynamics of Global Plate Motions*, vol. 121 of *Geophysical Monograph Series* (eds Richards, M. A., Gordon, R. G. & van der Hilst, R. D.) 377–398 (AGU, Washington DC, 2000).
17. Antretter, M., Riisager, P., Hall, S., Zhao, X. & Steinberger, B. in *Origin and Evolution of the Ontong Java Plateau* (eds Fitton, G., Mahoney, J., Wallace, P. & Saunders, A.) Geol. Soc. Lond. Spec. Pub. 229, 21–30 (2004).
18. Cande, S. C., Raymond, C. A., Stock, J. & Haxby, W. F. Geophysics of the Pitman Fracture Zone and Pacific–Antarctic plate motions during the Cenozoic. *Science* **270**, 947–953 (1995).
19. Cande, S. C., Stock, J. M., Mueller, R. D. & Ishihara, T. Cenozoic motion between East and West Antarctica. *Nature* **404**, 145–150 (2000).
20. Nankivell, A. P. *Tectonic Evolution of the Southern Ocean Between Antarctica, South America and Africa over the Past 84 Ma* Thesis, Univ. Oxford (1997).
21. Tikku, A. A. & Cande, S. C. On the fit of Broken Ridge and Kerguelen Plateau. *Earth Planet. Sci. Lett.* **180**, 117–132 (2000).
22. Gaina, C. *et al.* The tectonic history of the Tasman Sea; a puzzle with 13 pieces. *J. Geophys. Res.* **103**, 12413–12433 (1998).
23. Sutherland, R. The Australia–Pacific boundary and Cenozoic plate motions in the SW Pacific; some constraints from Geosat data. *Tectonics* **14**, 819–831 (1995).
24. Wood, R. A., Lamarche, G., Herzer, R. H., Delteil, J. & Davy, B. Paleogene seafloor spreading in the southeast Tasman Sea. *Tectonics* **15**, 966–975 (1996).
25. King, P. R. & Thrasher, G. P. *Cretaceous–Cenozoic Geology and Petroleum Systems of the Taranaki Basin, New Zealand* (Institute of Geological and Nuclear Sciences Monograph 13, Lower Hutt, New Zealand, 1996).
26. Heinemann, J. *et al.* Constraints on the proposed Marie Byrd Land–Bellingshausen plate boundary from seismic reflection data. *J. Geophys. Res.* **104**, 25321–25330 (1999).
27. Raymond, C. A., Stock, J. M. & Cande, S. C. in *The History and Dynamics of Global Plate Motions*, vol. 121 of *Geophysical Monograph Series* (eds Richards, M. A., Gordon, R. G. & van der Hilst, R. D.) 359–376 (AGU, Washington DC, 2000).
28. Sleep, N. H. Ridge-crossing mantle plumes and gaps in tracks. *Geochem. Geophys. Geosyst.* **3**, 8505 doi:10.1029/2001GC000290 (2002).
29. Ebinger, C. & Sleep, N. Cenozoic magmatism throughout east Africa resulting from impact of one large plume. *Nature* **395**, 788–791 (1998).
30. Behrendt, J. C. *et al.* Geophysical studies of the west Antarctic rift arm. *Tectonics* **10**, 1257–1273 (1991).
31. Cooper, A. K., Barker, P. F. & Brancolini, G. E. *Geology and Seismic Stratigraphy of the Antarctic margin*, vol. 68 of *Antarctic Research Series* (AGU, Washington DC, 1995).
32. McCarron, J. J. & Larter, R. D. Late Cretaceous to early Tertiary subduction history of the Antarctic Peninsula. *J. Geol. Soc. Lond.* **155**, 255–268 (1998).
33. Storey, B. C. & Nell, P. A. R. Role of strike-slip faulting in the tectonic evolution of the Antarctic Peninsula. *J. Geol. Soc. Lond.* **145**, 333–337 (1988).
34. Marks, K. M. & Stock, J. M. Early Tertiary gravity field reconstructions of the Southwest Pacific. *Earth Planet. Sci. Lett.* **152**, 267–274 (1997).
35. Sutherland, R. Basement geology and tectonic development of the greater New Zealand region: an interpretation from regional magnetic data. *Tectonophysics* **308**, 341–362 (1999).
36. Laird, M. G. in *South Pacific Sedimentary Basins*, vol. 2 of *Sedimentary Basins of the World* (ed. Ballance, P. F.) 37–49 (Elsevier, Amsterdam, 1993).
37. Cook, R. A., Sutherland, R. & Zhu, H. *Cretaceous–Cenozoic Geology and Petroleum Systems of the Great South Basin, New Zealand* (Institute of Geological and Nuclear Sciences Monograph 20, Lower Hutt, New Zealand, 1999).
38. Stock, J. & Molnar, P. Revised history of early Tertiary plate motion in the south-west Pacific. *Nature* **325**, 495–499 (1987).
39. Dick, H. J. B., Lin, J. & Schouten, H. An ultraslow-spreading class of ocean ridge. *Nature* **426**, 405–412 (2003).
40. Molnar, P. Continental tectonics in the aftermath of plate tectonics. *Nature* **335**, 131–137 (1988).
41. Hall, C. E., Gurnis, M., Sdrolias, M., Lavier, L. L. & Mueller, R. D. Catastrophic initiation of subduction following forced convergence across fracture zones. *Earth Planet. Sci. Lett.* **212**, 15–30 (2003).
42. Zatman, S., Gordon, R. G. & Richards, M. A. Analytic models for the dynamics of diffuse oceanic plate boundaries. *Geophys. J. Int.* **145**, 145–156 (2001).
43. Wessel, P. & Smith, W. H. F. Free software helps map and display data. *Eos* **72**, 441 (1991).
44. Sandwell, D. T. & Smith, W. H. F. Marine gravity anomaly from Geosat and ERS 1 satellite altimetry. *J. Geophys. Res.* **102**, 10039–10054 (1997).
45. Watts, A. B., Weisell, J. K., Duncan, R. A. & Larson, R. L. Origin of the Louisville Ridge and its relationship to the Eltanin Fracture Zone System. *J. Geophys. Res.* **93**, 3051–3077 (1988).
46. Koppers, A. A. P., Duncan, R. A. & Steinberger, B. The implications of a non-linear $^{40}\text{Ar}/^{39}\text{Ar}$ age progression along the Louisville seamount trail for models of fixed and moving hotspots. *Geochem. Geophys. Geosyst.* **5** doi:10.1029/2003GC000671 (2004).
47. Duncan, R. A. & Hargraves, R. B. $^{40}\text{Ar}/^{39}\text{Ar}$ geochronology of basement rocks from the Mascarene Plateau, Chagos Bank and the Maldive Ridge. *Proc. Ocean Drill. Program Sci. Res.* **115**, 43–51 (1990).
48. Hofmann, C., Féraud, G. & Courtillot, V. $^{40}\text{Ar}/^{39}\text{Ar}$ dating of mineral separates and whole rocks from the Western Ghats lava pile: further constraints on the duration and age of the Deccan Traps. *Earth Planet. Sci. Lett.* **180**, 13–27 (2000).
49. O'Connor, J. M. & le Roex, A. P. South Atlantic hot spot–plume systems: 1. Distribution of volcanism in time and space. *Earth Planet. Sci. Lett.* **113**, 343–364 (1992).
50. O'Connor, J. M. & Duncan, R. A. Evolution of the Walvis Ridge – Rio Grande Rise hot-spot system: Implications for African and South American plate motions over plumes. *J. Geophys. Res.* **95**, 17475–17502 (1990).

Supplementary Information accompanies the paper on www.nature.com/nature.

Acknowledgements We thank P. Molnar, J. Stock, T.H. Torsvik and R.A. Duncan for comments on the manuscript, and N. Sleep for a review. R.S. was supported by the NZ Foundation for Research Science and Technology, the Marsden Fund, and a Caltech Visiting Associate award. R.J.O. received support from the NSF.

Competing interests statement The authors declare that they have no competing financial interests.

Correspondence and requests for materials should be addressed to B.S. (bernhard.steinberger@uni-bayreuth.de).